Apparent exponents for the chain length dependence of the volume fraction in critical polymer solutions

Leonid V. Yelash and Thomas Kraska[a)]
Institut für Physikalische Chemie, Universität zu Köln, Luxemburger Straße 116, D-50939 Köln, Germany

Attila R. Imre
KFKI Atomic Energy Research Institute, H-1525 Budapest, P.O. Box 49, Hungary

Sylwester J. Rzoska
Institute of Physics, Silesian University, ul. Universytecha 4, 40-007, Katowice, Poland

(Received 1 October 2002; accepted 10 January 2003)

The dependence of the critical volume fraction at constant pressure as a function of the chain length of a polymer/solvent system can be described by a power law. The exponent of this power law is investigated based on an equation of state model and experimental data for various chain-molecule solutions here. The results are compared to recent molecular simulation data taken from the literature and analytical models. The theoretical models, simulation, and experimental data show that the exponent depends on the chain length of the dissolved chain molecules. The power law with a constant exponent is therefore not a universal relationship for this dependence. Based on the investigation of the chain length dependence a correlation for the critical volume fraction is proposed here. This function generalizes the Flory and a renormalization group model and is applied to the correlation of the experimental data. This more general relationship includes the power law with the exponent obtained from the Flory theory as limiting behavior. Some additional experimental data for oligomer solutions which are necessary for an investigation of the short chain length limit have been measured. © *2003 American Institute of Physics.*
[DOI: 10.1063/1.1557432]

I. INTRODUCTION

The interest in the chain length-dependent behavior of the critical properties of polymers is twofold. The fundamental aim is to understand how the critical properties are affected by molecular properties. It is of academic interest to explore universal relations such as power laws with universal exponents. Polymers are suitable for such study because their properties can be varied nearly continuously by variation of the chain length. Furthermore, the attraction parameters can be varied by choosing copolymers with periodic order. For example, a $-$ABABAB$-$copolymer can be regarded as a polymer of effective AB monomers with the corresponding effective interaction parameters. This makes it possible to vary attraction parameters as well as the chain length. A powerful method to access the topological transitions of the phase behavior of mixtures in the space of variable molecular interaction parameters is the global phase diagram method. In recent papers, global phase diagrams have been investigated for polymer solutions[1] and for polymer blends.[2] Here, we focus on the effect of chain length on the critical properties of polymer solutions. With new experimental data, new calculations with an equation of state based on a molecular-level approach, and molecular simulation data obtained from a literature review, here we discuss the chain length dependence of the critical properties and the exponent for the chain length dependence of the critical volume fraction.

The second objective of this work is based on the understanding of the phase behavior, to develop a method for the correlation and the extrapolation of the critical properties as function of the chain length. Such correlation should include the short and the long chain length limit. This is important for the prediction of critical properties for systems which have not been measured. Especially long chain molecules or high weight molecules are nonvolatile, and the determination of their properties such as saturation pressure is difficult.[3,4] Furthermore, due to chemical instability it is not possible to reach the critical temperature for several substances. However, for many chemical engineering correlation methods it is necessary to obtain the properties of the critical point even though it is chemically unstable. For such cases an extrapolation method is required which is based on a few available experimental data. Similarly, binary critical points in solutions of very high molecular weight polymers often need to be estimated from the few data available for solutions of lower molecular weight polymers.

A schematic representation of the liquid–liquid equilibrium in binary polymer solutions is shown in Fig. 1 for solutions of monodisperse polymers. The single-phase and two-phase regions are separated by coexistence curves (or cloud point curves in the case of polydisperse polymers). Weakly interacting polymer solutions such as the polystyrene/cyclohexane system can exhibit two separate coexistence curves. One is at low temperature with an upper critical solution point (UCST) at the maximum; the second is at high temperature with a lower critical solution temperature

a)Electronic mail: t.kraska@uni-koeln.de

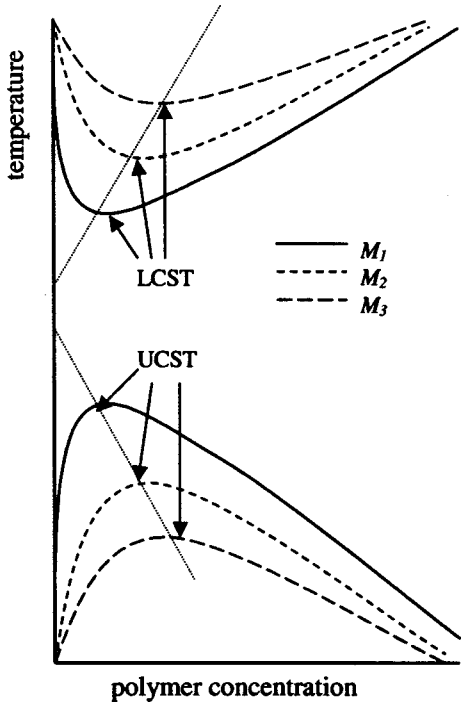

FIG. 1. Schematic representation of the liquid–liquid equilibrium in binary polymer solutions with three different molecular weights ($M_1>M_2>M_3$). The critical points—upper critical solution temperatures (UCST) and lower critical solution temperatures (LCST)—are marked by arrows. The dotted lines roughly represent the molecular weight dependence of the critical points.

(LCST) at the minimum. This is again valid for the monodisperse case. The concentrations corresponding to the upper and lower critical points are the critical concentrations. Figure 1 shows that the symmetry of the coexistence curves as well as the critical concentration depend on the molecular weight of the dissolved polymer.

The low temperature liquid–liquid equilibrium with a UCST in polymer solutions and blends can be described by the theory of Flory and Huggins.[5] The critical volume fraction depends on the molecular weight or the chain length in polymer systems as

$$\phi_c=\frac{\sqrt{N_1}}{\sqrt{N_1}+\sqrt{N_2}}. \tag{1}$$

Here, N_1 and N_2 are the number of repeating units of the polymers, and ϕ_c is the critical volume fraction of polymer 2. For $N=N_2/N_1$ one obtains the corresponding equation for a polymer solution in a small-molecule solvent

$$\phi_c=\frac{1}{1+\sqrt{N}}. \tag{2}$$

This equation is based on the assumption that the solvent is chemically of the same kind as the repeating unit of the polymer. Furthermore, it is assumed that N is given by the ratio of the molar volumes of substance 1 and 2 rather than the real chain length. In this definition it is possible to go experimentally below $N=1$ when the molar volume of the monomer is smaller than the molar volume of the solvent. In the limit of infinite chain length, the critical volume fraction can be described as function of the chain length by a power law

$$\phi_c=AN^r. \tag{3}$$

Here, A is a substance-dependent parameter. This power law should be distinguished from the power laws describing the near-critical behavior of a fluid. The value of the exponent r can be obtained by Flory theory in the limit of infinite chain length as $r=-0.5$.[5,6] Using renormalization arguments, de Gennes also suggested $r=-0.5$.[7] Later Muthukumar included three-body interactions and obtained the limiting value $r=-1/3$.[8] For high molecular weight polymers ranging from a few ten thousands to few million amu, one obtains experimental r values around -0.37 to -0.4.[9–13] For shorter chain molecules the values of r are usually closer to zero.

Povodyrev *et al.*[14] have replaced the exponent r in Eq. (3) by an effective exponent r_{eff} which is given for the Flory model by

$$r_{\mathrm{eff}}=-\frac{\sqrt{N}}{2(1+\sqrt{N})}. \tag{4}$$

This effective exponent r_{eff} has two limiting values: $r_{\mathrm{eff}}=-1/2$ for $N\to\infty$ and $r_{\mathrm{eff}}=-1/4$ for $N=1$. Experimental results for n-alkane solutions yield r values which are above $-1/4$ in the monomer limit, as shown in Table I. In real substances approaching the monomer limit, the chain-end effects become significant, which can cause this deviation. Additionally, in some n-alkane solutions such as the n-alkane/diethyl maleate systems, the value for N in terms of the ratio of the molar volumes can go below 1.

Computer simulations of short chain molecules also yield values deviating from the Flory limiting value. Until recent years it was not possible to simulate systems with very long chain molecules. Wilding *et al.*[15] obtained $r=-0.37$, Panagiotopoulos *et al.*[16] obtained $r=-0.36\pm0.02$ and $r=-0.39\pm0.02$ in two different simulations, Mackie *et al.*[17] obtained $r=-0.32$. Frauenkron and Grassberger[18] obtained an effective $r=-0.38$ for chains with up to 2048 units. Very recently, long chain systems were simulated by Yan and de Pablo[19] with up to 16 000 units, and they obtained an extrapolated value for r around the theoretically expected value of -0.5 using a generalized Flory equation for the correlation of ϕ_c as function of the chain length

$$\phi_c=\frac{1}{k_1+k_2N^{k_3}}. \tag{5}$$

For shorter chain length ($N=2000$) they obtained value $k_3=0.38$. Here, k_3 is an adjustable parameter which is related to the exponent by $r=-\lim_{N\to\infty}k_3$ in the long chain length limit.

Alternatively to Eq. (3), one can define a power law for the ratio of the polymer and the solvent volume fraction[20]

$$\frac{\phi_c}{1-\phi_c}=AN^{r_2}. \tag{6}$$

Inserting Eq. (2) into Eq. (6) yields the value $r_2=-0.5$ not only in the long chain length limit but for all chain lengths for the Flory model. This might suggest that Eq. (6) is a more appropriate definition for a power law.

Experimentally obtained values for r_2 are usually around -0.4 in several systems such as polystyrene/cyclohexane, polystyrene/methylcyclohexane, polymethylmetacrylate/3-octanone, n-alkane/nitrobenzene, n-alkane/dimethylacetamide, and n-alkane/diethyl maleate.[21] Analyzing literature data together with a few previously unpublished data for n-alkane solutions such as n-alkane/nitrobenzene, one can see that the r_2 values for short chains are around -0.4 for some systems within an experimental error. However, for the n-alkane/o-nitrotoluene and n-alkane/1-nitropropane systems the value appears to deviate. An overview over several experimental data is given in Table I. The value $r_2=-0.4$ is thought to be a universal value.[21] However, this assumption still has no theoretical background besides the observation that within the Flory theory the exponent r_2 is not a limiting value but valid for all chain lengths as mentioned above.

Most theories predict $r=-0.5$ in the long chain length limit, but the question remains how long a chain should be to be long enough? Experimentally, a few millions amu (or Dalton) is considered as high molecular weight (M); therefore, one might expect the value -0.5 for r or r_2. However, the experimental r and r_2 usually do not reach the limiting values for the studied long chain solutions even for high molecular weight (Table I). Based on a renormalization group analysis, a new dependence has been proposed[18,22,23]

$$\phi_c=\frac{\sqrt{\ln(N)}}{\sqrt{N}}. \tag{7}$$

This model yields the limiting values $r=-0.5$ and $r_2=-0.5$ for infinite N. At finite chain length, a value of -0.4 can be obtained as in the Flory model but in a different chain length range. Similar dependence has been found by Yan and de Pablo[19] for their simulation data. They found linear dependence of $N\phi_c^2$ on $\ln(N)$.

There are several reasons why experimental and theoretical exponents can differ. These can be systematic and experimental uncertainties.

Systematic errors are, for example, the effect of the polydispersity which is not known about much in this context. Most theories describe the N dependence for monodisperse polymer solutions. In experiments, polymers with $M_w/M_n<1.06$ are considered as nearly monodisperse, but the remaining polydispersity and the corresponding moments of the molecular weight distribution can affect the exponent. According to the recent experimental and theoretical results of de Sousa and Rebelo,[24] increasing polydispersity has a small but nonvanishing effect on the critical concentration which decreases. Additionally, Šolc *et al.*[25] predicted that polydisperse polymers may have nonzero ϕ_c in the infinite long chain length limit, which cannot be described by Eqs. (1)–(4).

Furthermore, the end-group effect can cause a systematic error which can affect the chain length dependence at short chain length. It is known that the phase behavior of short chain molecules including oligomers is influenced crucially by end groups.[26] However, in the long chain length limit this effect vanishes.

According to Singh and Van Hook[27] the equal-volume criterion which is frequently used for determining ϕ_c, contains uncertainties. These authors predicted only very minor deviation in the resulting experimental data. However, this deviation can become crucial for small ϕ_c values which can affect the values of the exponents in the long chain length limit.

Other sources of discrepancies are experimental uncertainties. The calculation of the volume fraction from the weight fraction requires the densities of the substances. These densities are measured at room temperature and in some cases used for the calculation of the volume fraction at higher temperature. However, considering the small difference in the density at these temperatures, this effect is expected to be small.

There are also limitations in the theory employed for the investigation of the exponents. Lattice models such as the Flory model usually do not include a variable density. In real systems the density depends on the state conditions such as temperature. Furthermore, in theoretical approaches such as lattice models, equation of state models or simulation models, the repeating units of a real polymer are approximated by united atom or coarse grain approaches. In such approximation a group of atoms or repeating units are placed on a lattice site or are represented by a sphere in a chain. In the context of these simplifications it is necessary to establish a relation between the real and the model units. Another limitation can be that a model is valid only for chemically identical solvent molecules and chain segments. This is the case in some lattice models but usually not in equation of state models.

II. METHOD OF INVESTIGATION

A. Experiment

In this work we compare experimental data with theoretical investigation. Most of the analyzed data are taken from the literature.[12,13,28–57] Some nitrobenzene/n-alkanes systems were measured in this work (Table II). These data complete the data available in the literature and are required in the context of this investigation. The critical composition is determined from the volume ratio of the two separated phases, which is about unity at the critical point. This phase separation can take hours or even days; the temperature has to be held at a constant value (within 0.1 K) during the whole separation process. Phase volumes are recorded when the meniscus between the two liquids is sharp. For details about the experimental method the reader is referred to Ref. 58.

B. Theory

In order to investigate the exponents of the critical volume fraction, we have employed an equation of state model for long chain molecules including polymers. This classical mean field model has been described in the literature in detail[1] and has also been applied to phase equilibria investigation of polymer blends.[2] Here, it is summarized briefly.

TABLE I. Experimentally obtained exponents for the UCST.

Chain molecules	Solvents	M range of chain molecules	N range of chain molecules (with and without end-groups)	N range as molar volume ratio[a]	$-r$ (for N with endgroups and as molar volume ratio)	$-r_2$ (for N with endgroups and as molar volume ratio)	Validity of Eq. (7) (R of linear fit of $N\phi_c^2$ and $\ln N$) [number of points]	Data obtained from references
n-alkanes	N,N-dimethylacetamide	72.15–128.28	5–9/3–7	1.8–2.8	0.152±0.005 0.205±0.006	0.40±0.01 0.54±0.01	0.9991 [5] 0.9996	[20]
n-alkanes	Nitrobenzene	72.15–282.55	5–20/3–18	1.12–3.48	0.19±0.02 0.23±0.02	0.42±0.04 0.52±0.04	[8] 0.9881	[45, 51], this paper
n-alkanes	o-nitrotoluene	72.15–226.45	5–16/3–14	0.98–2.48	0.13±0.01 0.16±0.01	0.31±0.02 0.38±0.03	0.9986 [10] 0.9992	[44, 45]
n-alkanes	1-nitropropane	142.28–226.45	10–16/8–14	2.2–3.3	0.27±0.08 0.31±0.09	0.64±0.19 0.74±0.23	0.8616 [5] 0.8664	[45]
n-alkane	Diethyl maleate	86.18–156.31	6–11/5–9	0.81–1.31	0.188±0.002 0.240±0.006	0.43±0.01 0.55±0.02	0.9995 [6] 0.9998	[48, 50, 52–54, 56]
Polystyrene[b,d]	Nitroethane	13 000–130 000	125–1250	172.3–1723	0.22±0.04	0.26±0.05	0.9841 [4]	[57]
Polystyrene[b,d]	Cyclohexane	35 000–330 0000	337–31 700	305–29 100	0.38±0.02	0.41±0.02	0.7867 [40]	[13, 28–35, 37, 40–43, 49]
Polystyrene[b,d]	Methylcyclo-hexane	9000–1 260 000	86–12 115	67–9411	0.37±0.01	0.41±0.01	0.9203 [28]	[36, 38, 39, 55]
Polybutadiene[c,d]	n-Propyl acetate	61 000–823 000	1130–15 241	596–8041	0.43±0.01	…	…	[47]
Polymethyl-methacrylate[b,d]	3-octatnone	21 600–225 900	216–2259	117–1219	0.38±0.01	0.41±0.01	0.9847 [10]	[12, 46]

[a]Molar volume of the chain component divided by the molar volume of the solvent.
[b]Some PS data were given in mass fraction, volume fraction was calculated by using 1.05 g/cm^3 average density for PS.
[c]For Polybutadiene/n-Propyl acetate system only r exponent was given, without the experimental data. This system was excluded from our further analysis, because the critical concentration was taken as the concentraction corresponding to the maxima of the cloud point curves assuming monodispersity.
[d]For polymers, M_w was used instead of N, but both being big enough, it does not make any difference. For example, in polystyrene/nitroethane (in this case polymer chains are relatively short) using M_w instead of N makes only 0.01 difference in the exponents.

TABLE II. Experimental data for nitrobenzene/n-alkane systems.

Carbon number	Critical temperature (K)	Critical volume fraction (V_{alk}/V_{nb})
5	292.95	0.627
9	294.11	0.597
11	298.27	0.573
16	309.15	0.506
18	314.89	0.513
20	319.15	0.485

The advantage of such equation of state model is to have a tool to calculate critical data for a model system which then can be employed for the investigation of chain-length-dependent phenomena. Furthermore, an equation of state model includes a variable density and allows one to vary molecular properties expressed by the equation of state parameters.

The equation of state model is derived in the framework of molecular thermodynamics[1] based on the first order thermodynamic perturbation theory of Wertheim[59] and of Chapman *et al.*[60] The underlying molecular model is a chain molecule consisting of tangential hard spheres with the hard sphere fluid as reference model. Furthermore, the van der Waals dispersion term has been employed. The reason for choosing this term is its simplicity, theoretical basis, and ability to represent the main physical effects. The equation employed here has been derived based on an approach of mapping molecular properties onto a mathematically simplified equation of state.[61–63] The resulting equation of state is fourth order in the density.[64]

$$p=\frac{RT}{V_m}\left(\frac{3+Ay+By^2}{(1-y)(3-4y)}\right)-\frac{16a_{seg}}{b^2}y^2, \tag{8}$$

$$A=\frac{2-30m+48cm}{4}, \tag{9}$$

$$B=\frac{-21+37m+8cm}{4}, \tag{10}$$

$$y=\frac{mb}{4V_m}. \tag{11}$$

Here, a_{seg} is the van der Waals attraction parameter and b the covolume parameter for a repeating unit, c an entropic coefficient, and m the chain length parameter of the tangential-sphere model. These parameters have been correlated[64] to the critical data of the homologous series of the n-alkane from methane to n-triacontane. We choose to calculate the parameters a and b for methane with $m=1$ and $c=1$. Hence, all dependences of the parameters on the number of carbon atoms N are correlated with the chain length parameter m and the entropic coefficient c. The model parameter m represents the number of tangential spheres, while the real segments are better represented by fused spheres. As noted earlier, in most molecular simulations as well as in lattice models, the model chain length parameters are not identical with the number of repeating units in real molecules. The relations between the real number of repeating units N, the corresponding number of tangential spheres m, and the entropic factor cm within this model are given below

$$m=1+0.3770(N-1)+0.2660\frac{N-1}{N}, \tag{12}$$

$$cm=1+0.3426(N-1)-0.4212\frac{N-1}{N}. \tag{13}$$

The mixing rules for the extension of the equation of state is based on the Flory model[64] with the volume fraction rather than on the mole fraction x_i

$$b=\frac{x_1m_1b_1+x_2m_2b_2}{x_1m_1+x_2m_2}, \tag{14}$$

$$c=\frac{x_1m_1c_1+x_2m_2c_2}{x_1m_1+x_2m_2}, \tag{15}$$

$$a_{seg}=\frac{x_1^2m_1^2a_{11}+2x_1m_1x_2m_2a_{12}+x_2^2m_2^2a_{22}}{(x_1m_1+x_2m_2)^2}, \tag{16}$$

$$m=x_1m_1+x_2m_2. \tag{17}$$

In this work we investigate polymer solutions for which we set m_1 to unity and vary only m_2 for $b_1=b_2$.

The binary systems are calculated for different sets of interaction parameters a_{ij} here. A convenient way of presenting the effects of different attraction parameters on the phase behavior is a global phase diagram as introduced by van Konynenburg and Scott.[65,66] This method has been further developed by several authors in recent years[64,67–71] and also applied to address problems in phase behavior of polymer mixtures.[1,2] In such diagrams, boundary curves between different kinds of phase diagram are calculated in the space of the molecular parameters. These are, for example, the phase diagram types IV and type II separated by a tricritical boundary state. Type IV exhibits a UCST and a LCST while type II exhibits an UCST only. The coordinates of global phase diagrams are reduced dimensionless values of the equation of state parameters. In this work, only the attraction parameters are varied. The definitions as given below are valid for $b_1=b_2=b_{12}$

$$\zeta=\frac{a_{22}-a_{11}}{a_{22}+a_{11}}, \tag{18}$$

$$\lambda=\frac{a_{22}-2a_{12}+a_{11}}{a_{22}+a_{11}}. \tag{19}$$

In practice, usually λ–ζ sections of the global phase diagram are calculated in which each point represents one binary system determined by a set of the three interaction parameters a_{11}, a_{22}, a_{12}. The boundary states are higher-order thermodynamic states such as tricritical states which serve as transition states between two types of phase behavior. The just-mentioned tricritical state is a boundary between phase diagrams with a continuous binary critical curve and critical curve which is interrupted by a three-phase line.

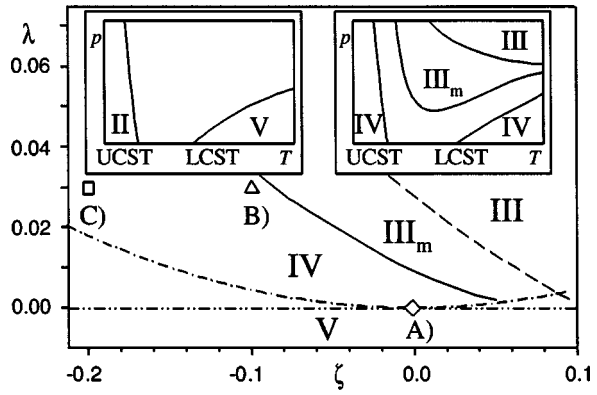

FIG. 2. Global phase diagram of the investigated polymer/solvent model systems. This global phase diagram is calculated for the solvent/1000-mer system and represents roughly the global phase diagram in the long chain length limit. The further shift of the boundary curves to the left-bottom corner is small for polymer chain length beyond $N=1000$ and can be neglected. Square, triangle, and diamond mark the interaction parameters of the systems investigated here. Solid curve: double critical end point boundary; dashed curve: critical pressure step point boundary separating types III and III_m; dashed-dot-dot curve: arithmetic mean of the cross-attraction parameter; dashed-dot: geometric mean for the cross-attraction parameter. The inset shows the binary critical curves for the phase diagram types schematically. The solid curves in the inset are binary critical curves such as the UCST or LCST curves. Type II phase behavior is not present in the range of the parameters λ and ζ shown here.

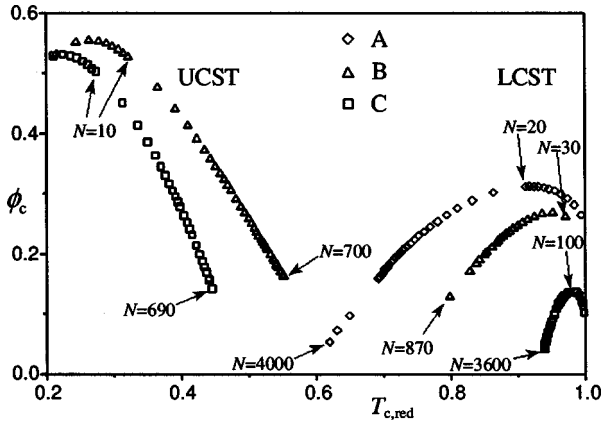

FIG. 3. Critical solution temperatures as function of the volume fraction calculated at constant pressure for the three systems A, B, and C marked in Fig. 2.

III. RESULTS

For the calculation of the exponents r and r_2 as function of the chain length, we have set the pressure constant to the critical pressure of the solvent and calculated critical points for monodisperse polymer solutions. The critical pressure of many solvents is usually on the order of a few MPa. Experiments are usually performed at a pressure of 1 bar. It has been shown[2] that the difference in pressure under given conditions has only a small influence on the critical composition. Furthermore, in the context of this work we have checked the influence of the pressure on the exponent r and found it to be negligible. The calculations have been performed for different sets of interaction parameters a_{ij} using the equation of state model described above. In Fig. 2 the three interaction parameter sets A, B, and C are marked in a global phase diagram for the 1000-mer/solvent systems. This corresponds, for example, to a solution of polystyrene with $M_w \approx 100\,000$ g/mol in cyclohexane. With increasing chain length, the positions of these three systems in the global phase diagram remain unchanged, while the boundary curves move further down to lower λ and ζ values. The knowledge of the global phase diagram is very important in this investigation because we have to make sure that in the course of increasing the polymer chain length no topological change in the phase behavior appears as, for example, from type IV to III_m. Such transition is physically possible, for example, in the systems polystyrene/acetone or polystyrene/nitroethane. However, here we want to exclude such transition because it would lead to nonreliable results with respect to the exponents. From the investigation of the global phase diagram we know the location of the boundary curves for long chain length polymer solutions.[1] The shift of the boundary curves, which represent such topological changes in the binary phase diagrams, slows down with increasing chain length and reaches a limit. This limit is approximated by the 1000-mer/solvent case (Fig. 2). Hence, we can be sure that the phase diagram types remain unchanged with changing chain length for selected sets of attraction parameters.

For these systems the critical volume fraction is calculated at fixed pressure as function of the chain length N of the polymer. Since we intend to compare the results to experimental data, we use the definition of the volume fraction which is based on the number of repeating units N $\phi_i = x_i N_i b_i / (x_1 N_1 b_1 + x_2 N_2 b_2)$. Here, only systems with equal segment covolumes $b_1 = b_2$ are considered. Therefore, ϕ_c simplifies to the segment fraction $\phi_i = x_i N_i / (x_1 N_1 + x_2 N_2)$. The resulting values for the critical volume fraction as function of the chain length are shown in Fig. 3 as $\phi_c - T_c$ diagram. The curves represent three selected different systems A, B, and C, which differ in the attraction parameters of the solvent–solvent, the solvent–segment, and the segment–segment interaction. System A has a cross-attraction parameter which is given by the geometric mean of the solvent–solvent and the segment–segment attraction parameters. System B has a cross-attraction parameter which is smaller than the geometric mean. It is, furthermore, close to a boundary state, the double critical end point, which can affect its phase behavior. At such double critical end point the UCST and the LCST branches merge, i.e., a type IV system turns into a type III_m system (Fig. 1). System C is at more negative ζ values which correspond to significantly different solvent–solvent and segment–segment interactions. The three curves at higher temperature shown in Fig. 3 are lower critical solution temperature (LCST) states at constant pressure, and the two curves at lower temperature are upper critical solution temperature (UCST) states. Here, system A is a type V system with the global interaction parameters $\lambda = 0.0$ and $\zeta = 0.0$ (Fig. 2). Such type exhibits only an LCST. Systems B and C are type IV systems with different interaction parameters $\lambda = 0.03$, $\zeta = -0.1$ and $\lambda = 0.03$, $\zeta = -0.2$, respectively. Type IV systems have a LCST and an UCST. The corresponding pT diagrams are shown schematically in the inset in Fig. 2.

The Flory theory[5] predicts a linear dependence of $1/T_c$

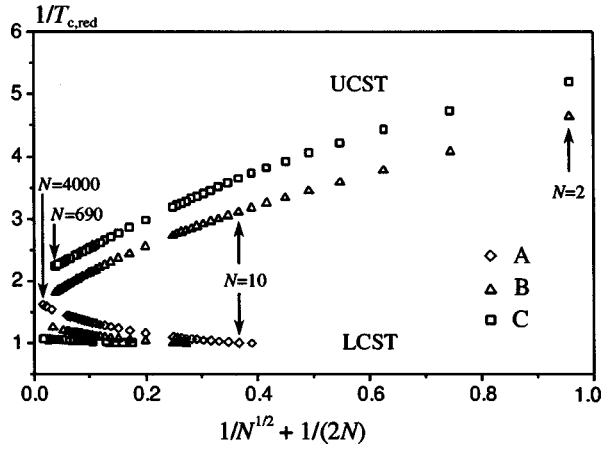

FIG. 4. Flory–Schultz plot for the model systems investigated here. In the limit $N\rightarrow\infty$ the data tend to a linear dependence. Here $T_{c,red}$ is the liquid–liquid critical temperature of the solution reduced by the liquid–vapor critical temperature of the solvent.

as function of $1/N^{1/2}+1/(2N)$ in the long chain length limit. Here T_c is the liquid–liquid critical temperature of the solution. This dependence is known as a Flory–Schultz plot. In Fig. 4 the Flory–Schultz plot of the critical curves is shown for the systems investigated here. One can see that the equation of state model employed here tends to linear behavior for the UCST. In our calculations as well as for experimental data,[72,73] this linearity holds down to approximately $N=10$. For the LCST this seems to be the case in the long chain length limit only.

In Fig. 5 the calculated critical points are plotted in a $\log(\phi_c)$–$\log(N)$ diagram. Such plot is usually employed for the determination of the exponent r from experimental data; r is given as the slope of the data in this plot. The topology of most curves is similar in Fig. 5. The slope is positive for small chain length and changes to negative values beyond a maximum at higher N. With further increasing chain length

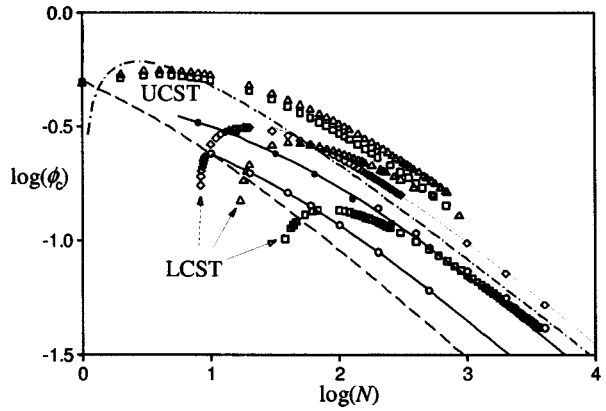

FIG. 5. Double logarithmic plot of the critical mole fraction as function of the chain length N. The symbols (except circles) are the USCT and LCST, which are upper and lower liquid–liquid critical points, calculated with the equation of state. The simulation data (Refs. 15,19) (open circles) (Ref. 18) (filled circles), the Flory model (dashed curve), and the renormalization group model (dot-dashed curve) are added for the UCST. The data are correlated by a Flory-type function Eq. (20) in order to guide the eye. The LCST vanishes at a certain small value or N because the phase diagram type changes from IV to II with decreasing N values.

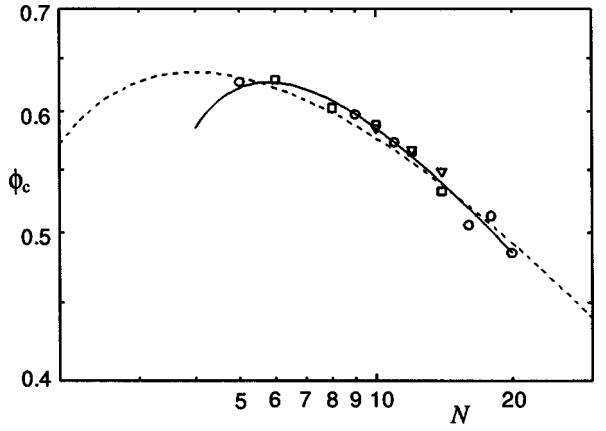

FIG. 6. Experimental data of the UCST for the family of nitrobenzene/n-alkane systems. Circles: this work; squares: literature data (Ref. 45); triangles: literature data (Ref. 51). The curves are correlations by Eq. (21). The obtained parameters are $P_1=-0.425$, $P_2=-1.746$, $P_3=1.871$ (solid curve) and if forced to positive values $P_1=0.752$, $P_2=0.0$, $P_3=2.209$ (dashed curve), which reduces Eq. (21) to a two-parameter equation.

the curves tend to flatten out. This tendency can also be observed for the experimental data for the n-alkane/nitrobenzene systems as shown in Fig. 6. The curves calculated with our model show quantitatively different behavior for the UCST and the LCST. The maximum for the UCST is very flat while it is pronounced for the LCST. In addition to the calculations with the equation of state model, other functions and data taken from the literature are plotted. These are the Flory function,[52] the molecular simulation data of Grassberger and Frauenkron,[18] a renormalization group model taken from the same authors, and Monte Carlo simulation data of Yan and de Pablo *et al.*[19] These curves are interpolated here by a generalized Flory function

$$\phi_c=\frac{1}{k_1+k_2\sqrt{N}}, \tag{20}$$

which has exponent $r=-0.5$ in the long chain limit. With these models, only the UCST is investigated. To the best of our knowledge there are no data for the exponent of the LCST in the literature. One can see that the Flory function exhibits no maximum. Simulation data[15,18,19] suggest a flat maximum similar to the equation of state calculations for the UCST curves. The renormalization group model exhibits a pronounced maximum at short chain length which is similar to our calculations for the LCST curves.

It is not possible to determine whether the exponent reaches a constant values in the long chain limit because of the curvature in the $\log(N)$–$\log(\phi_c)$ plot. Therefore, we plot in Fig. 7 the calculated exponents r for the models and data as function of the chain length $\log(N)$. The exponents calculated from literature data and data presented here for various systems are listed in Table I. The exponent calculated with the Flory model rapidly approaches its long chain-length limit at $r=-0.5$. The Flory function has a similar curvature as the experimental systems; however, the absolute values are quite different. The renormalization group model and the simulation data of Grassberger and Frauenkron are closer to the experimental data. The renormalization group model ap-

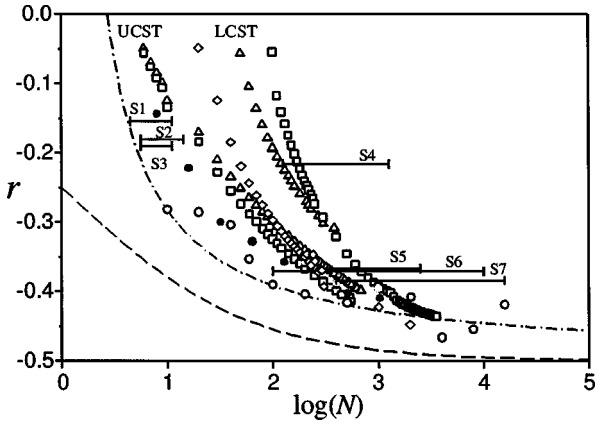

FIG. 7. Calculation of the exponent r according to Eq. (3) for all models shown in Fig. 5. In addition experimental data for the UCST are added. Experimental systems: S1: n-alkanes/N,N-dimethylacetamide; S2: n-alkanes/nitrobenzene S3: n-alkanes/dimethyl maleate; S4: polystyrene/nitroethane; S5: PMMA/3-octanone S6: polystyrene/methylcyclohexane; S7: polystyrene/cyclohexane. For the legend see Fig. 5.

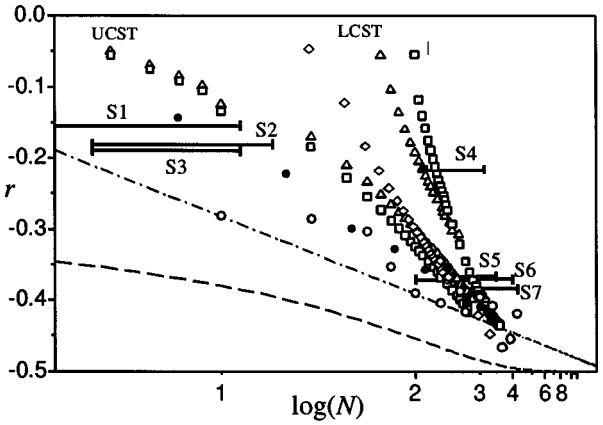

FIG. 9. Extrapolation of the exponent r to long chain length. The abscissa is plotted in reciprocal units. For the legend see Figs. 5 and 6.

proaches the Flory limit but much slower than the Flory function. In the monomer limit, the Flory function [see Eq. (2)] and the renormalization group model [see Eq. (7)] show different behavior. While the Flory function ends at a value of $r=-0.25$, the renormalization group model goes to positive values. This reflects that the Flory function does not exhibit a maximum in the $\log(\phi_c)$–$\log(N)$ plot (Fig. 5). The exponent r of the renormalization group model diverges to infinity in the monomer limit due to the logarithmic correction. However, it should be noted that the renormalization group model was derived in the limit of infinitely long chain molecules and does not implicitly include the monomer limit.

In order to address the question whether Eq. (4) is a more suitable definition of the power law than Eq. (3), we have plotted in Fig. 8 the values for the exponent r_2 as function of $\log(N)$. The Flory model yields, as mentioned earlier, a constant value of $r_2=-0.5$. The renormalization group model approaches a region around the value $r_2=-0.5$ faster than for r, but it exhibits an oscillation around this value and converges then to the limiting value $r_2=-0.5$. The effective values for the exponent r_2 calculated with the equation of state model behave similar as the corresponding values for r shown in Fig. 7, with the exception that the limiting value of r_2 is approached faster. The same is true for the simulation data. The experimental results, simulation data, and the equations of state calculations for the UCST for long chain molecules are in agreement. In addition, with the equation of state model it is possible to calculate the exponents for the LCST.

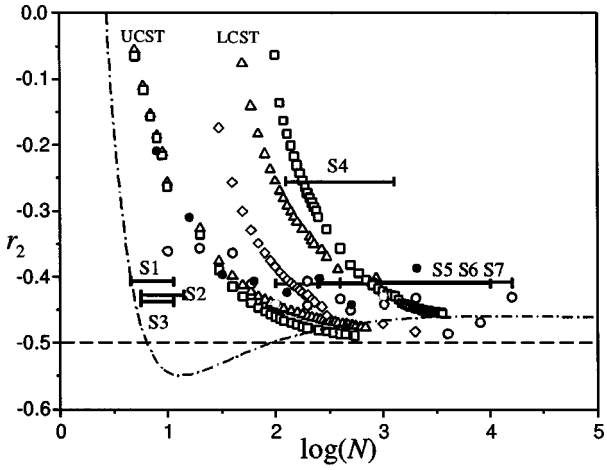

FIG. 8. Calculation of the exponent r_2 according to Eq. (4) for all models shown in Fig. 5. For legend see Figs. 5 and 6.

From the analysis of the exponents r and r_2 calculated as function of the chain length, it appears that the exponents obtained in experiments are rather apparent exponents than the limiting exponent as obtained by the Flory model. Nevertheless, the question remains whether all these functions contain the Flory value as limiting value or if they suggest another limiting value. In order to investigate the long chain limit, we have replotted Fig. 7 with reciprocal $\log(N)$ axis in Fig. 9. Such plot makes it possible to estimate the limiting values more accurately. We found that all models and data seem to converge to the same limiting value given by the Flory model for r.

The exponents for systems A, B, and C calculated here with an equation of state model are in the range of the experimental data, although somewhat shifted to higher N values. One can see that the exponent r depends on the chain length. Hence, the exponents obtained in experiments by linear regression are apparent exponents. This is due to the nonlinear dependence of $\log(\phi_c)$ on $\log(N)$ as shown in Figs. 5 and 6. Topologically the values of these exponents can cross zero with decreasing chain length. This shows that a power law with a constant exponents does not represent the universal behavior of the critical volume fraction as function of the chain length. Therefore, it is necessary to find a function type other than the power law. It appears that the generalized Flory function given by Eq. (20) does not sufficiently cover all features of the chain length dependence of the UCST and the LCST. While the UCST exhibits a finite value behavior in the short chain length limit, the LCST seems to diverge. Actually, the LCST can vanish with decreasing N which is related to the change in phase behavior from type IV such as the polystyrene/cylohexane system to II

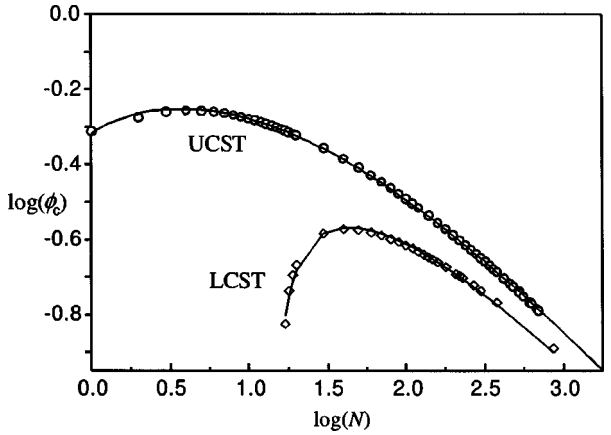

FIG. 10. Correlation of LSCT and UCST data of system B (see Fig. 2) with Eq. (21). The parameters for the LCST are $P_1=0.694$, $P_2=-9.443$, $P_3=3.536$, and for the UCST the parameters are $P_1=3.017$, $P_2=3.742$, $P_3=2.982$.

such as the polystyrene/dioctyl phtalate system.[72] This would be then the short chain length limit of the exponent. In the long chain length limit the experimental data as well as calculations rather agree with the renormalization group model. We suggest a correlation with three parameters which combines the generalized Flory function [Eq. (20)] with the renormalization group model [Eq. (7)][74]

$$\phi_c=\frac{\sqrt{P_2+P_3\ln(N)}}{P_1+\sqrt{N}}. \tag{21}$$

This equation can be rewritten by introducing $u=\log(\phi_c)$ and $v=\log(N)$, which makes it suitable for the correlation of data in the $\log(\phi_c)$–$\log(N)$ plot

$$u=\log\left(\frac{\sqrt{P_2+P_3 v\ \ln(10)}}{P_1+\sqrt{10^v}}\right). \tag{22}$$

For the parameter set $P_1=0$, $P_2=0$, $P_3=1$ one can recover the renormalization group model; for $P_1=1$, $P_2=1$, $P_3=0$ one obtains the Flory model. The equation for the chain length dependence of the exponent r corresponding to Eq. (21) is given by

$$r=\frac{1}{2}\left(\frac{1}{\frac{P_2}{P_3}+\ln(N)}-\frac{\sqrt{N}}{P_1+\sqrt{N}}\right). \tag{23}$$

This equation can be used together with the power law given by Eq. (1). In Fig. 10 the correlations of equation of state data for system B, which is a type IV system with UCST and LCST, are shown in the $\log(\phi_c)$–$\log(N)$ plot. The corresponding adjusted parameters are given in the caption of Fig. 10. The data calculated with equation of state are free of experimental uncertainties and exhibit no scattering. Hence, they are suitable for preliminary testing a correlation equation before applying it to experimental data. Equation (21) appears to be suitable for the correlation of the different chain length dependence of the LCST and the UCST. This equation can also be useful for the correlation of experimental data instead of using Eq. (3) which yields a linear function in the $\log(\phi_c)$–$\log(N)$ plot. Further advantage of the correlation with Eq. (21) is its ability for extrapolation towards the long chain length limit. Once the parameters of Eq. (21) are obtained, one can calculate the apparent exponent with Eq. (23).

A function based on a similar idea has been proposed independently recently by Anisimov *et al.*[75] While their function includes the long chain length limit it does not include the short chain length limit, e.g., it has a maximum in the $\log(\phi_c)$–$\log(N)$ plot at around $N=1$. Our aim here is to include both limits, which is possible with Eq. (21).

Inspection of the values of the correlated parameters shows that the parameter P_2 is different for different types of chain length behavior of the critical volume fraction. For the UCST P_2 is usually positive while it is usually negative for the LCST. A negative value for P_2 can lead to an undefined volume fraction for solutions of short chain molecules. This corresponds to the fact that for such systems the LCST can be absent due to a topological change in the phase diagram at short chain length. The value of P_3 is similar for the UCST and the LCST. The value of P_1 differs: it is high for the UCST and low for the LCST. However, based on these observations we do not claim a physical meaning of these parameters.

In Fig. 6 the correlation of the experimental data for the series nitrobenzen/n-alkanes is shown. We applied Eq. (21) to experimental data taken from the literature supplemented by our own data. One can see that Eq. (21) is suitable to correlate the critical volume fraction against the chain length. Two sets of parameters have been chosen, both of which have a maximum at short chain length. The first three-parameter set contains one negative parameter P_2. In the second correlation all parameters are forced to positive values. The best correlation for this case is obtained for $P_2=0$, which reduces Eq. (21) to a two-parameter equation at the expense of accuracy.

IV. CONCLUSIONS

The investigation with an equation of state model accomplished here shows that the exponents of the power laws describing the chain length dependence of the critical volume fraction in polymer solutions depend on the chain length. This is true for both definitions of the power law given by Eqs. (3) and (4). The evaluation of analytical models such as the Flory model and a renormalization group model exhibits the same trend as the equation of state model. The equation of state model, lattice models, simulation and experimental data agree with respect to the trend of the apparent exponent and the limiting value for infinite chain length. Some drawbacks of the analytical models which are based on lattice models can be overcome by equation of state models.

With respect to the above-mentioned power law, we have found two effects which are possible explanations for the difference between the experimental and Flory exponents. Based on the calculations, one can show that the experimentally obtained exponents are apparent exponents. They can change depending on the chain length range of the

polymer investigated. Only an apparent value of the exponent r can be obtained from experimental data when forcing a linear fit onto an actually nonlinear dataset. The problem is that the experimental error margin of the data in typical experiments is too large to recognize the often very low curvature in the $\log(\phi_c)$–$\log(N)$ plot. The correlation proposed here [Eqs. (21)–(23)] captures this curvature and can be useful in applications to experimental data.

ACKNOWLEDGMENTS

This work was partially supported by the Hungarian Science Foundation (OTKA) under Contract Number F 034333, by the German Science Foundation (DFG) and the Funds of the German Chemical Industry. A.R.I. was also supported by a Bolyai Research Fellowship. The authors also acknowledge the support by a joint grant of the German Science Foundation and the Hungarian Academy of Science.

[1] L. V. Yelash and T. Kraska, Phys. Chem. Chem. Phys. **1**, 2449 (1999).
[2] A. R. Imre, T. Kraska, and L. V. Yelash, Phys. Chem. Chem. Phys. **4**, 992 (2002).
[3] T. Kraska, K. O. Leonhard, D. Tuma, and G. M. Schneider, Fluid Phase Equilib. **194–197**, 469 (2002).
[4] T. Kraska, K. O. Leonhard, D. Tuma, and G. M. Schneider, J. Supercrit. Fluids **23**, 209 (2002).
[5] P. J. Flory, *Principles of Polymer Chemistry* (Cornell University Press, Ithaca, 1953), Chap. XIII.
[6] I. C. Sanchez, Macromolecules **17**, 967 (1984).
[7] P. G. de Gennes, *Scaling Concepts in Polymer Physics* (Cornell University Press, Ithaca, 1979), Chap. 4, Sec. 3.
[8] M. Muthukumar, J. Chem. Phys. **85**, 4722 (1986).
[9] R. Perzynski, M. Delsanti, and M. Adam, J. Phys. (France) **48**, 115 (1987).
[10] Yu. B. Melnichenko, V. V. Klepko, and V. V. Shilov, Polymer **29**, 1010 (1988).
[11] B. Chu, K. Linliu, P. Xie, Q. Ying, Z. Wang, and J. W. Shook, Rev. Sci. Instrum. **62**, 2252 (1991).
[12] K. Q. Xia, C. Franck, and B. Widom, J. Chem. Phys. **97**, 1446 (1992).
[13] C. L. Caylor and B. M. Law, J. Chem. Phys. **104**, 2070 (1996).
[14] A. A. Povodyrev, M. A. Anisimov, and J. V. Sengers, Physica A **264**, 345 (1999).
[15] N. Wilding, M. Müller, and K. J. Binder, Chem. Phys. **105**, 802 (1996).
[16] A. Z. Panagiotopoulos, V. Wong, and M. A. Floriano, Macromolecules **31**, 912 (1998).
[17] A. D. Mackie, A. Z. Panagiotopoulos, and S. K. Kumar, J. Chem. Phys. **102**, 1014 (1995).
[18] H. Frauenkron and P. Grassberger, J. Chem. Phys. **107**, 9599 (1997).
[19] Q. Yan and J. J. de Pablo, J. Chem. Phys. **113**, 5954 (2000).
[20] X. An, H. Zhao, F. Jiang, and W. Shen, J. Chem. Thermodyn. **28**, 1221 (1996).
[21] X. An, F. Jiang, C. Chen, and W. Shen, Pure Appl. Chem. **70**, 609 (1998).
[22] B. Duplantier, J. Phys. (France) **43**, 991 (1982).
[23] J. S. Hager, M. A. Anisimov, J. V. Sengers, and E. E. Gorodetskii, J. Chem. Phys. **117**, 5940 (2002).
[24] H. C. de Sousa and L. P. N. Rebelo, J. Polym. Sci., Part B: Polym. Phys. **36**, 632 (2000).
[25] K. Šolc, K. Dusek, R. Koningsveld, and H. Berghmans, Collect. Czech. Chem. Commun. **60**, 1661 (1995).
[26] A. R. Imre and W. A. Van Hook, Macromolecules **33**, 5308 (2000).
[27] R. R. Singh and W. A. Van Hook, J. Chem. Phys. **87**, 6088 (1987).
[28] R. Koningsveld, L. A. Kleintjens, and A. R. Shultz, J. Polym. Sci., Part A-2 **8**, 1261 (1970).
[29] Th. G. Scholte, J. Polym. Sci., Part A-2 **9**, 1553 (1971).
[30] Th. G. Scholte, J. Polym. Sci. C **39**, 281 (1972).
[31] N. Kuwahara, M. Nakata, and M. Kaneko, Polymer **14**, 415 (1973).
[32] M. Nakata, N. Kuwahara, and M. Kaneko, J. Chem. Phys. **62**, 4278 (1975).
[33] B. A. Wolf and M. C. Sezen, Macromolecules **10**, 1010 (1977).
[34] M. Nakata, T. Dobashi, N. Kuwahara, M. Kaneko, and B. Chu, Phys. Rev. A **18**, 2683 (1978).
[35] N. Hamano, M. Kuwahara, and M. Kaneko, Phys. Rev. A **20**, 1135 (1979).
[36] T. Dobashi, M. Nakata, and M. Kaneko, J. Chem. Phys. **72**, 6685 (1980).
[37] J. Hashizume, A. Teramoto, and H. Fujita, J. Polym. Sci., Part B: Polym. Phys. **19**, 1405 (1981).
[38] K. Shinozaki, T. van Tan, Y. Saito, and T. Nose, Polymer **23**, 728 (1982).
[39] T. Dobashi, M. Nakata, and M. Kaneko, J. Chem. Phys. **80**, 948 (1984).
[40] M. Tsuyumoto, Y. Einaga, and H. Fujita, Polym. J. (Tokyo) **16**, 229 (1984).
[41] G. Schmitz, H. Klein, and D. Woermann, Z. Naturforsch., A: Phys. Sci. **43A**, 825 (1988).
[42] W. A. Goedel, A. Zielesny, L. Belkoura, T. Engels, and D. Woermann, Ber. Bunsenges. Phys. Chem. **94**, 17 (1990).
[43] H. Yoshizaki and R. Kono, Mem. Natl. Def. Acad. Japan **31**, 61 (1992).
[44] M. Sliwinska-Bartkowiak, J. Phys.: Condens. Matter **5**, 407 (1993).
[45] P. Urbanowicz, S. J. Rzoska, M. Paluch, B. Sawiczki, A. Szulc, and A. Zioło, J. Chem. Phys. **201**, 575 (1995).
[46] K. Q. Xia, X. Q. An, and W. G. Shen, J. Chem. Phys. **105**, 6018 (1996).
[47] H. J. Lee and I. H. Parl, Macromolecules **33**, 4983 (2000).
[48] X. An, X. Liu, and W. Shen, J. Chem. Thermodyn. **29**, 669 (1997).
[49] S. A. Vshivkov and A. P. Safranov, Macromol. Chem. Phys. **198**, 3015 (1997).
[50] X. An, X. Cui, T. Wang, and W. Shen, J. Chem. Thermodyn. **30**, 1199 (1998).
[51] X. An, F. Jiang, and W. Shen, J. Chem. Soc., Faraday Trans. **94**, 2169 (1998).
[52] X. An, C. Mao, G. H. Sun, and W. Shen, J. Chem. Thermodyn. **30**, 689 (1998).
[53] X. An, J. Yang, and W. Shen, J. Chem. Thermodyn. **30**, 13 (1998).
[54] X. An, J. Yang, and W. Shen, J. Chem. Thermodyn. **30**, 1253 (1998).
[55] X. An, K. Q. Xia, W. Shen, and X. L. Oiu, J. Chem. Phys. **111**, 8298 (1999).
[56] X. An, X. Cui, and W. Shen, J. Chem. Thermodyn. **32**, 187 (2000).
[57] H. C. de Sousa and L. P. N. Rebelo, J. Chem. Thermodyn. **32**, 355 (2000).
[58] R. Koningsveld, W. H. Stockmayer, and E. Nies, *Polymer Phase Diagrams* (Oxford University Press, New York, 2001).
[59] M. Wertheim, J. Chem. Phys. **87**, 7323 (1987).
[60] W. G. Chapman, G. Jackson, and K. E. Gubbins, Mol. Phys. **65**, 1057 (1988).
[61] L. V. Yelash and T. Kraska, Phys. Chem. Chem. Phys. **2**, 4734 (2000).
[62] L. V. Yelash and T. Kraska, Fluid Phase Equilib. **182**, 27 (2000).
[63] L. V. Yelash, T. Kraska, E. A. Müller, and N. F. Carnahan, Phys. Chem. Chem. Phys. **1**, 4919 (1999).
[64] L. V. Yelash and T. Kraska, Phys. Chem. Chem. Phys. **1**, 4315 (1999).
[65] R. L. Scott and P. H. van Konynenburg, Discuss. Faraday Soc. **49**, 87 (1970).
[66] P. H. van Konynenburg and R. L. Scott, Philos. Trans. **298A**, 495 (1980).
[67] D. Furman and R. B. Griffiths, Phys. Rev. A **17**, 1139 (1978).
[68] L. V. Yelash and T. Kraska, Ber. Bunsenges. Phys. Chem. **102**, 213 (1998).
[69] T. Kraska and U. K. Deiters, J. Chem. Phys. **96**, 539 (1992).
[70] T. Kraska, Ber. Bunsenges. Phys. Chem. **100**, 1318 (1996).
[71] I. Polishuk, J. Wisniak, H. Segura, L. V. Yelash, and T. Kraska, Fluid Phase Equilib. **172**, 1 (2000).
[72] A. R. Imre and W. A. Van Hook, J. Phys. Chem. Ref. Data **25**, 637 (1996); **25**, 1277 (1996).
[73] A. R. Imre and W. A. Van Hook, J. Polym. Sci., Part B: Polym. Phys. **25**, 637 (1996).
[74] L. V. Yelash, T. Kraska, A. R. Imre, and S. L. Rzoska, Proceedings of the Jülich Soft Matter Days (2001).
[75] M. A. Anisimov, A. F. Kostko, and J. V. Sengers, Phys. Rev. E **65**, 051805 (2002).